to carbon. The excitation energies of benzene[31] are 460 kJ mol^{-1} for the singlet and 351 kJ mol^{-1} for the triplet. As observed, homolytic excited-state bond cleavage should not occur.[4,5]

A second example is the free-radical chlorination of hydrocarbons by protonated *N*-chloroamines of which the intramolecular example is the Hofmann-Loffler-Freytag reaction.[32] Although there has been considerable dispute about the mechanism of these processes, it now appears to be well established that the critical chain-propagating step is hydrogen abstraction, often at a 2° carbon, by the radical cation of an amine (eq 13) Values of the

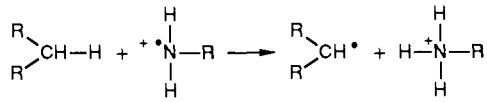
(13)

BDE[29] for $(CH_3)_2CH-H$, 358 kJ mol^{-1}, and $H-N(CH_3)_2$, 383 kJ mol^{-1}, indicate that this step would be mildly exothermic for the neutral aminyl radical (eq 14). Protonation of the nitrogen increases the N-H bond strength and makes the step in eq 13 much more favorable.


(14)

As a third example,[13] we note the gas-phase elimination of H_2 from CH_3XH^+ (eq 15). In all cases, estimation of the activation

$$CH_3XH^+ \rightarrow CH_2X^+ + H_2 \qquad X = NH_2, OH, F, SH \qquad (15)$$

energy for this process gives lower values than that calculated in this paper for homolytic cleavage of the strong C-X bonds.

Although our discussion has focused on the energetics of protonation, it is interesting to consider the changes, δr, in A-B bond lengths due to protonation. The data in Table III indicate that the trends for bond lengths are similar to those for bond dissociation energies. For example, δr, like $\delta\Delta$, increases along the series $CH_3-NH_2/CH_3-N^+H_3$, $CH_3-OH/CH_3-O^+H_2$, CH_3-F/CH_3-F^+H. In general, protonation leads to an increase in the A-B bond length, with three exceptions being noted among the HF/6-31G*-optimized structures included in this paper. Two of the three cases correspond to the two cases for which $\delta\Delta$ is also negative (see Table II). Normally, bond lengths decrease as bond strengths increase, and in fact correlations have been made between the shortening of bond lengths and the electronegativity difference of bonded atoms.[33] Although we do not have an explanation for this observation, the rather unusual lengthening of bonds despite the increased electronegativity is likely due to the positive charge on the heteroatom. The geometries of three of the pairs of molecules have been optimized using the MP2 method. The results listed in Table III indicate that including the effects of electron correlation does not alter the qualitative trends and, therefore, we conclude that the HF/6-31G*-optimized structures are sufficiently accurate for the present purposes.

Note Added in Proof. After this paper was accepted for publication we learned from Professor D. R. Arnold of a similar discussion of the relationship between bond dissociation energies and the electronegativity of charged atoms.[34]

Acknowledgment. We thank William Brandon for some preliminary calculations and the Natural Sciences and Engineering Research Council of Canada for financial assistance.

(32) Tanner, D. D.; Arhart, R. *Tetrahedron* **1985**, *41*, 4261, and references therein.

(33) Reference 19; pp 228-230.
(34) Williams, T. F. *J. Am. Chem. Soc.* **1962**, *84*, 2895.

Molecular Dynamics Simulations of α-D-Glucose in Aqueous Solution

J. W. Brady

Contribution from the Department of Food Science, Stocking Hall, Cornell University, Ithaca, New York 14853. *Received October 27, 1988*

Abstract: Molecular dynamics simulations have been performed for an aqueous solution of α-D-glucopyranose. A single glucose molecule was modeled surrounded by 207 SPC water molecules using periodic boundary conditions in the microcanonical ensemble. Solvation was found to have little effect upon the dynamically averaged structure of the sugar molecule. Transitions in the orientations of the various carbohydrate hydroxyl groups, which were found to be extremely unlikely in vacuo, occurred easily in solution, although the rotational motions were damped by the solvent. The exocyclic hydroxymethyl group unexpectedly rotated spontaneously to the trans-gauche (TG) conformation early in the simulation and remained in this orientation for the remainder of the calculation. The structuring of the water molecules around the C2 hydroxyl group was found to be substantially perturbed for some orientations of this group relative to the anomeric hydroxyl group. This perturbation may be the result of inadequate averaging due to the simulation time scale or, if real, could be related to the basis for the differing anomeric concentrations at equilibrium.

I. Introduction

It is now generally understood that the conformational structure and dynamics of biopolymers are strongly influenced by aqueous solvation. Unfortunately, the role of water in these biological systems is not simple or easily generalized. The special behavior of aqueous systems, arising from the unique molecular structure and hydrogen-bonding properties of water, makes dielectric continuum models of aqueous solutions inadequate for understanding many important properties of biological molecules in solution. Furthermore, the complex chemical structure of most biological solutes makes such systems particularly difficult to treat theoretically; often quite different functional groups, such as nonpolar aliphatic groups and hydrogen-bonding dipoles, are juxtaposed in close spatial proximity in molecules such as peptides or nucleic acids. Fortunately, with the advent of high-speed computers, it is becoming feasible to use techniques such as Monte Carlo and molecular dynamics simulations[1-3] to directly model

(1) Brooks, C. L.; Karplus, M.; Pettitt, B. M. Proteins: A Theoretical Perspective of Dynamics, Structure, and Thermodynamics. *Advances in Chemical Physics* Wiley-Interscience: New York, 1988; Vol. LXXI.
(2) Karplus, M.; McCammon, J. A. *Annu. Rev. Biochem.* **1983**, *53*, 263.

0002-7863/89/1511-5155$01.50/0

the behavior of aqueous solutions. A number of important aqueous systems have now been studied using these techniques, including simple nonpolar molecules,[4-6] ions,[7,8] methanol,[9] *tert*-butyl alcohol,[10] urea,[11,12] the alanine "dipeptide" (*N*-methylalanylacetamide),[13,14] and even entire proteins.[15] Much of our understanding of the detailed molecular behavior of such solutions comes from these simulations.

Because of the significant role of carbohydrates in many biological systems, particularly in molecular recognition processes such as blood group incompatibility, cell attachment and bonding, antigenicity, and viral infection, understanding the aqueous solvation behavior of carbohydrate polymers is also of considerable importance. Complex solution behavior might well be expected in the case of carbohydrates, including the pyranoid ring forms of the simple sugars. These molecules contain many adjacent alcohol groups held in approximately fixed relative orientations by the geometry of the sugar ring (usually a cyclohexane-like "chair"), as well as nonpolar centers (CH and CH_2 groups) and ether-like ring oxygen atoms. The series of hexose monosaccharides illustrates the resulting complex solvation behavior; these molecules are essentially all structural isomers differing only in the stereochemical configurations about the asymmetric carbon atoms of the ring, yet their properties in aqueous solution, such as their equilibrium anomeric ratios, are distinct.[16,17]

Currently there are no adequate theoretical models to describe the behavior of carbohydrates and polyols in aqueous solution.[17] It has been suggested that the anomeric equilibrium is the result of intramolecular quantum mechanical effects such as a possible unfavorable dipole–dipole interaction between equatorial anomeric hydroxyl groups and the ring oxygen. However, such models are unable to rationalize the differing anomeric preferences of glucose and mannose in aqueous solution or the dependence of these ratios upon solvent characteristics. Furthermore, molecular mechanics calculations which do not include a potential energy term designed specifically to give the observed anomeric ratio have found little potential energy difference between pyranoid sugar anomers.[18,19] It has thus also been proposed that much of the anomeric preference of monosaccharides may be determined by solvation effects.[17] A model of pyranoid solvation has been advanced, which assumes that axial hydroxyl groups are less favorably hydrated than are equatorial ones.[20,21] This theory is based upon the observation that in β-D-glucose, the hydroxyl oxygen atoms are disposed about the ring at essentially the same positions as the oxygen atoms of water molecules in a chair of water molecules taken from a tridymite ice lattice and spaced with the distance between next nearest oxygens being 4.9 Å, the second nearest neighbor distance in liquid water. In this model, then, β-D-glucopyranose comfortably "fits" into a slightly expanded ice lattice as a model of the liquid phase, while the axial hydroxyl of α-D-glucopyranose does not. Older versions of this model seem to assume a more extended icelike structuring in liquid water than has been observed from simulations,[22] but the idea of differing compatibilities of axial and equatorial hydrogen-bonding patterns with their surroundings may nonetheless be valid. While there is currently no experimental way to directly test such a model, it may be possible to use numerical simulations to examine the molecular basis of the aqueous solvation of monosaccharides.

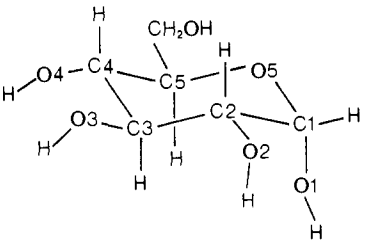

Figure 1. α-D-Glucopyranose in the $^4C_1$ conformation.

Molecular mechanics calculations have long been applied to carbohydrate molecules,[23] and recently there have been several studies of the dynamics of simple carbohydrates using molecular dynamics simulations.[19,24-31] These studies have begun to provide considerable information about the flexibility and conformational fluctuations of these molecules. Unfortunately, most calculations to date have been of carbohydrate molecules in vacuo, due to the much lower cost of vacuum computer simulations; only the Koehler et al. studies of cyclodextrin crystals[30,31] and the Post et al. study of the lysozyme–substrate complex[24] have included crystallographic water molecules. Vacuum and crystal studies alone clearly cannot adequately illuminate the effects of solvation upon carbohydrates. For this reason, further dynamics simulations that explicitly include aqueous solvent molecules would be most useful. Such a molecular dynamics simulation is reported here of a system consisting of α-D-glucopyranose (Figure 1) in aqueous solution to examine some of these effects of solvation upon sugar behavior and to investigate the nature of sugar hydration.

II. Procedures

In the simulation reported here Newton's equations of motion were integrated numerically for every atom in a model system using the general molecular mechanics program CHARMM developed by Karplus and co-workers.[32] The system consisted of a single α-D-glucopyranose molecule surrounded by water molecules in a cubic primary box subject to periodic boundary conditions to eliminate edge effects. The potential energy function used was a typical CHARMM-type molecular mechanics energy function,[32] with the solute parameters being a set recently developed for glucose from vibrational and crystallographic data,[33] using atomic partial charge values similar to those found by Jorgensen to be suitable for condensed phase simulations.[34] These charges are larger than those that have typically been used in the past for molecular mechanics studies of carbohydrates, and this may lead to an overemphasis of intramolecular hydrogen bonding when used in vacuo (see below). The water molecules were modeled using the SPC potential function devel-

(3) McCammon, J. A.; Harvey, S. C. *Dynamics of Proteins and Nucleic Acids*; Cambridge University Press: Cambridge, 1987.
(4) Dashevsky, V. G.; Sarkisov, G. N. *Mol. Phys.* **1974**, *27*, 1272.
(5) Owicki, J. C.; Scheraga, H. A. *J. Am. Chem. Soc.* **1977**, *99*, 7413.
(6) Swaminathan, S.; Harrison, S. W.; Beveridge, D. L. *J. Am. Chem. Soc.* **1978**, *100*, 5705.
(7) Palinkas, G.; Riede, W. O.; Heinzinger, K. *Z. Naturforsch.* **1977**, *32A*, 1137.
(8) Dang, L. X.; Pettitt, B. M. *J. Chem. Phys.* **1987**, *86*, 6560.
(9) Okazaki, S.; Nakanishi, K.; Touhara, H. *J. Chem. Phys.* **1984**, *81*, 890.
(10) Tanaka, H.; Nakanishi, K.; Touhara, H. *J. Chem. Phys.* **1984**, *81*, 4065.
(11) Kuharski, R. A.; Rossky, P. J. *J. Am. Chem. Soc.* **1984**, *106*, 5794.
(12) Tanaka, H.; Nakanishi, K.; Touhara, H. *J. Chem. Phys.* **1985**, *82*, 5184.
(13) Rossky, P. J.; Karplus, M. *J. Am. Chem. Soc.* **1979**, *101*, 1913.
(14) Ravishanker, G.; Mezei, M.; Beveridge, D. L. *J. Comput. Chem.* **1986**, *7*, 345.
(15) Ahlström, P.; Teleman, O.; Jönsson, B. *J. Am. Chem. Soc.* **1988**, *110*, 4198.
(16) Suggett, A. In *Water: A Comprehensive Treatise*; Franks, F., Ed.; Plenum: New York, 1975; Vol. 4, pp 519–567.
(17) Franks, F. *Pure Appl. Chem.* **1987**, *59*, 1189.
(18) Dunfield, L. G.; Whittington, S. G. *J. Chem. Soc., Perkin Trans. 2* **1977**, 654.
(19) Brady, J. W. *Carbohydr. Res.* **1987**, *165*, 306.
(20) Kabayama, M. A.; Patterson, D. *Can. J. Chem.* **1958**, *36*, 563.
(21) Suggett, A. *J. Solution Chem.* **1976**, *5*, 33.
(22) Stillinger, F. H.; Rahman, A. *J. Chem. Phys.* **1974**, *60*, 1545.
(23) Brant, D. A. *Annu. Rev. Biophys. Bioeng.* **1972**, *1*, 369.
(24) Post, C. B.; Brooks, B. R.; Karplus, M.; Dobson, C. M.; Artymiuk, P. J.; Cheetham, J. C.; Phillips, D. C. *J. Mol. Biol.* **1986**, *190*, 455.
(25) Brady, J. W. *J. Am. Chem. Soc.* **1986**, *108*, 8153.
(26) Prabhakaran, M.; Harvey, S. C. *Biopolymers* **1987**, *26*, 1087.
(27) Homans, S. W.; Pastore, A.; Dwek, R. A.; Rademacher, T. W. *Biochemistry* **1987**, *26*, 6649.
(28) Ha, S. N.; Madsen, L. J.; Brady, J. W. *Biopolymers* **1988**, *27*, 1927.
(29) Tran, V.; Brady, J. W. *Biopolymers*, in press.
(30) Koehler, J. E. H.; Saenger, W.; van Gunsteren, W. F. *Eur. Biophys. J.* **1987**, *15*, 197.
(31) Koehler, J. E. H.; Saenger, W.; van Gunsteren, W. F. *Eur. Biophys. J.* **1987**, *15*, 211.
(32) Brooks, B. R.; Bruccoleri, R. E.; Olafson, B. D.; States, D. J.; Swaminathan, S.; Karplus, M. *J. Comput. Chem.* **1983**, *4*, 187.
(33) Ha, S. N.; Giammona, A.; Field, M.; Brady, J. W. *Carbohydr. Res.* **1988**, *180*, 207.
(34) Jorgensen, W. L. *J. Am. Chem. Soc.* **1981**, *103*, 335; *Ibid.* **1981**, *103*, 341.

Table I. Comparison of the Dynamically Averaged Structure of α-D-Glucopyranose As Calculated from Vacuum and Solution Simulations[a]

angle	dynamical mean (vacuum)	rms fluct	dynamical mean (solution)	rms fluct	crystal
C1-C2-C3-C4	-53.0	5.7	-52.5	6.0	-51.3
C2-C3-C4-C5	53.6	5.9	52.5	6.2	53.3
C3-C4-C5-C6	-174.8	7.2	-176.1	6.7	-176.6
C3-C4-C5-O5	-52.9	6.0	-53.9	6.0	-57.5
C4-C5-O5-C1	57.2	5.9	59.7	5.7	62.2
C5-O5-C1-C2	-59.2	5.5	-60.2	5.6	-60.9
O5-C1-C2-C3	54.4	5.6	54.8	5.8	54.1
C1-C2-C3-O3	-175.4	6.5	-175.0	6.9	-172.0
C2-C3-C4-O4	175.3	6.6	175.6	6.8	175.3
O1-C1-C2-O2	55.2	7.5	58.5	7.8	56.9
O1-C1-C2-C3	-67.6	6.7	-66.2	6.9	-68.7
C1-C2-C3	109.2	3.4	109.7	3.1	111.1
C2-C3-C4	110.5	3.1	110.7	3.3	109.8
C3-C4-C5	112.5	3.1	110.3	3.2	111.1
C4-C5-C6	114.7	3.6	113.3	3.8	111.5
C4-C5-O5	111.7	2.8	109.8	2.8	108.7
C5-O5-C1	116.4	2.7	115.2	2.5	113.7
O5-C1-O1	107.3	3.0	108.6	2.9	111.5

[a] All angles are given in degrees.

oped by Berendsen and co-workers.[35] No explicit hydrogen bond function was employed in this force field; recent studies have indicated that hydrogen bonding can be adequately represented by Coulomb interactions using larger polar hydrogen and oxygen atomic partial charges as in the present study.[36] All hydrogen atoms were included explicitly in the simulations; that is, "united" or "extended" atom representations were not used.[32] Chemical bond lengths involving hydrogen atoms in both the solute and solvent were kept fixed throughout the simulation using the constraint algorithm SHAKE,[37] as were the bond angles for the solvent molecules.

The initial coordinates for the system were prepared by superimposing the crystallographic coordinates for α-D-glucopyranose[38] upon the coordinates of a well-"aged" cubic box of water molecules equilibrated in a previous simulation of pure SPC water. Those water molecules with oxygen atoms whose van der Waals radii overlapped any of the atoms in the glucose molecule were then discarded from the system, leaving 207 water molecules and 1 solute molecule. The box length was set at a value of 18.556 Å to give the desired density of 1.016 g/cm^3, the approximate density of a glucose solution of this weight percentage at room temperature. The concentration of the resulting solution was 0.26 M. Initial velocities for all atoms in the system were selected from a Boltzmann distribution at 300 K, the temperature at which the box of pure water was equilibrated, and their equations of motion were integrated using a Verlet algorithm[39] with a step size of 1 fs. The system was equilibrated for 10.2 ps to relax any artificial starting conditions produced by the initialization procedure, with periodic scaling of the atomic velocities during this period if the temperature deviated from the desired value of 300 K by more than an acceptable tolerance. Minimum image periodic boundary conditions were employed,[40] and interactions between molecules greater than 9.0 Å apart were truncated. Switching functions were used to make these long-range interactions go smoothly to 0 between separations of 7.0 and 8.5 Å.[32] In order to avoid artificially splitting dipoles in these long-range interactions, the switching was applied on a "group-by-group" rather than an "atom-by-atom" basis, with the groups corresponding to electrostatically neutral groups of atoms in the solute and to complete water molecules for the solvent. As is standard practice for periodic boundary conditions, molecules leaving the primary box across one face reentered on the opposite side. Interactions for each atom are thus summed over all of its near neighbors in the primary box and all those image neighbors that are within the cutoff distance. Following the equilibration period, the integration was continued without further interference for an additional 32-ps period of data collection. The system was well equilibrated and the energy adequately conserved during the integration, with no overall drift in the temperature or total energy. The total simulation required almost 40 CPU days of computer time on a DEC VAX 11/750 computer.

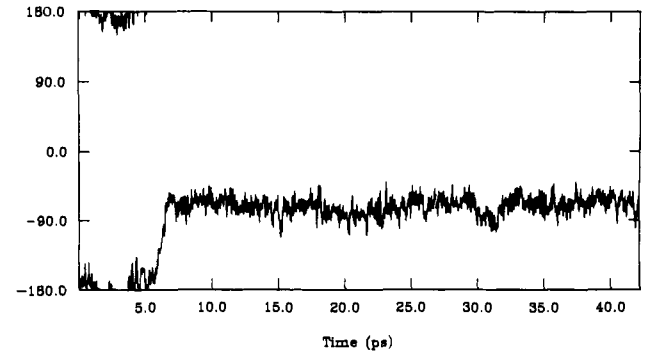

Figure 2. History of the dihedral angle C4-C5-C6-O6 describing the orientation of the exocyclic hydroxymethyl group for the entire simulation, including equilibration period.

III. Results and Discussion

The mean structure of the glucose ring in this simulation, as measured by its dynamically averaged torsion and bond angles, was found to be only slightly affected by the presence of aqueous solvent. Table I compares these dynamically averaged values for selected internal coordinates from the simulation to those computed in a previous study from an ensemble of vacuum trajectories using the same potential energy function[33] and to the crystal structure.[38] As can be seen, no significant shifts in ring geometry occurred upon solution, and many of the small shifts that did occur tended to bring the average structure closer to the experimental geometry. The rms fluctuations in these internal coordinates in the solution simulation were also similar to those observed in vacuo. It is quite likely that few of these differences are statistically significant. The mean value of the Cremer-Pople pucker parameter[41] Q averaged over the data collection period of this simulation was found to be 0.566 ± 0.035. The value of this coordinate was found to be 0.561 ± 0.034 when averaged over a similar vacuum trajectory, which was run for comparison purposes. The experimental value for this quantity for crystalline glucose, determined by X-ray diffraction, is 0.567, which is also the value in the energy-minimized structure in vacuo using the present potential energy function. The dynamically averaged value for the pucker parameter θ from the present solution simulation was found to be 8.28 ± 4.46° and 7.69 ± 3.64° for the comparison vacuum trajectory. The experimentally determined crystal value of this coordinate is 3.51°. Neither of these shifts represent a significant change in the overall magnitude or type of puckering of the pyranoid ring.

While the ring geometry was not significantly perturbed by solvation, there were significant conformational changes in the various exocyclic groups that occurred during the solution simulations. In the vacuum studies using this potential energy function, the exocyclic hydroxymethyl group was found to prefer the so-called trans-gauche (TG) orientation at a value of -60° for the C4-C5-C6-O6 torsion angle (with the O6 atom trans to O5 and gauche to C4) since this conformation allows the formation of an intramolecular hydrogen bond between the O6 and O4 hydroxyl groups. With the overemphasis on intramolecular hydrogen bonding in vacuo that presumably occurs with this potential energy function due to its use of larger atomic partial charges appropriate for condensed-phase conditions, this internal hydrogen bond causes the TG conformation to be strongly favored in vacuo. Surprisingly, this was also the conformation found throughout most of the present solution simulation. In this simulation, the exocyclic hydroxymethyl group underwent a spontaneous transition during the equilibration period from the crystallographic starting conformation (gauche-trans, GT) at 180° to the TG conformer.

(35) Berendsen, H. J. C.; Postma, J. P. M.; van Gunsteren, W. F.; Hermans, J. In *Intermolecular Forces*; Pullman, B., Ed.; Reidel: Dordrecht, The Netherlands, 1981; p 331.
(36) Reiher, W. E. Ph.D. Thesis, Harvard University, Cambridge, 1985; Reiher, W. E.; Karplus, M., to be submitted for publication.
(37) van Gunsteren, W. F.; Berendsen, H. J. C. *Mol. Phys.* **1977**, *34*, 1311.
(38) Brown, G. M.; Levy, H. A. *Science* **1965**, *147*, 1038; *Acta Crystallogr.* **1979**, *B35*, 656.
(39) Verlet, L. *Phys. Rev.* **1967**, *159*, 98.
(40) Metropolis, N.; Rosenbluth, A. W.; Rosenbluth, M. N.; Teller, A. H.; Teller, E. *J. Chem. Phys.* **1953**, *21*, 1087.
(41) Cremer, D.; Pople, J. A. *J. Am. Chem. Soc.* **1975**, *97*, 1354.

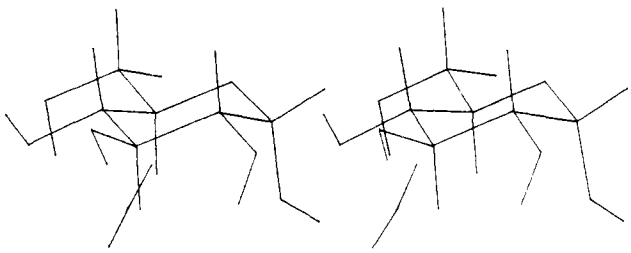

Figure 3. Stereoview of the final coordinate set for the glucose molecule and one selected water molecule hydrogen bonding to the O2 and O3 hydroxyl groups. The exocyclic hydroxymethyl group in this picture is in the trans-gauche (TG) conformation.

The history of the C4–C5–C6–O6 torsion angle for the entire 42 ps of simulation, including the equilibration period, is illustrated in Figure 2. Following this transition, the molecule remained in the TG conformation until the end of the simulation. In this TG conformation (illustrated in Figure 3 for a characteristic "snapshot" of the conformation, the final coordinate set of the trajectory), the O4–O6 hydrogen bond was present for the majority of the simulation, as in the vacuum case. This intramolecular hydrogen bond was disrupted by intermolecular hydrogen bonding with the solvent for only a few brief (1–2-ps) periods. The donating and accepting hydroxyls in the pair exchanged identities three times during the simulation.

The experimental distribution of rotamers in the simple sugars and their derivatives has been a subject of some disagreement. From NMR measurements of proton chemical shifts and coupling constants, it has been reported that for glucose in D_2O solution the TG conformer is not present to any large extent,[42-44] although an alternative interpretation of assignments for 2-acetamido-2-deoxy-D-glucose predicted the TG form to be a nonnegligable conformer.[45] The occurrence of this transition to the TG form during the equilibration phase of the present calculation could have been an artifact produced by large unphysical local temperature fluctuations such as can occur during equilibration. The subsequent stability of this conformation may then simply be the result of an activation barrier to rotations in solution and does not necessarily indicate that this conformer is the most stable for the system. The question of relative stability would require the observation of the partitioning resulting from many transitions in a much longer simulation or from numerous additional simulations. It should be noted, however, that during the present simulation the water molecules immediately adjacent to the O4, O6, and C6 groups exchanged several times and that both the O4 and O6 hydroxyl groups underwent several spontaneous rotations. It is thus also quite possible that the spontaneous occurrence and long persistence of the TG conformation in these simulations is an indication of the inadequacy of the potential energy function for describing the rotamer energies and barriers. The energy gain of the O4–O6 hydrogen bond may be partially offset by a "gauche effect"[46,47] between the C5–O5 and C6–O6 bonds in the actual molecule, which may need to be included in further revisions of this energy function.

In a previously reported series of simulations of α-D-glucose in vacuo[25] using an alternate potential energy function,[48] frequent and rapid transitions were observed in the positions of the various hydroxyl groups of the sugar (see Figure 5 of ref 25). In vacuum MD simulations of glucose using the present potential energy surface,[33] the enhanced hydroxyl dipoles result in the formation of intramolecular hydrogen bonds in the absence of alternate solvent hydrogen bond partners. The strength of these electrostatic interactions produces a circuit or ring of intramolecular hydrogen bonds, with each hydroxyl group forming a strained hydrogen bond to the adjacent group and with all of the OH bond vectors "pointing" in approximately the same direction, either counterclockwise or clockwise with respect to the direction of the numbering of the ring carbon atoms. The formation of such rings was observed in vacuum simulations of both α- and β-D-glucopyranose,[33] maltose,[28] and the glucose ring of sucrose[29] and has been reported experimentally from NMR studies of glucose, maltose, and sucrose[49,50] in crystals and dimethyl sulfoxide (DMSO) solution. The formation of such networks of hydrogen bonds in DMSO solution implies the existence of the TG exocyclic hydroxymethyl conformation in the presence of this solvent.

Because all of the hydrogen bonds in these structures point in the same direction around the ring, steric repulsions inhibit a single hydroxyl from flipping over to change its direction and hydrogen bond to the nearest hydroxyl in the other direction. If one of the hydroxyls changes direction, they all must, which means that in vacuo the activation energy for such a transition is quite large, since several hydrogen bonds must be simultaneously broken before the compensating opposite hydrogen bonds are formed. For this reason, reorientations of these hydroxyl groups are extremely rare in vacuum MD simulations with this potential energy function even though the energy difference between the two forms is small. In aqueous solution, however, the hydroxyls can hydrogen bond to the solvent water molecules, and changes in orientation of individual hydroxyl groups are facile and relatively uncorrelated. Such facile rotation has been observed experimentally for glucose in DMSO solution.[50] Figure 4 illustrates the histories of the torsion angles defining the orientations of these groups during the dynamics simulation. As can be seen from these figures, conformational transitions for these groups occurred throughout the simulation, although less frequently than in the vacuum simulations[25] using the Rasmussen potential energy function,[48] and in many cases much more slowly, as the solvent water molecules exert a significant frictional drag on these groups. This reorientational behavior indicates that the formation of stable, long-lived intramolecular circuits of hydrogen bonds observed in the vacuum simulations of glucose, maltose, and sucrose may not be representative of aqueous solution behavior.

As can be seen from Figure 4, some transitions in hydroxyl orientations during this simulation were as abrupt and rapid as those observed in the vacuum dynamics calculations,[25] while others occurred quite gradually, in some cases requiring many picoseconds to complete. Most of the groups exhibited both types of behavior, which is presumably strongly influenced by the behavior of the adjacent solvent molecules. Very little correlation in the reorientation of adjacent hydroxyl groups can be discerned from Figure 4. The orientation of the anomeric hydroxyl group was relatively stable in this study, undergoing only one transition late in the simulation (see discussion below). Because of the time lag, it is unclear whether this conformational change precipitated the subsequent transition in the orientation for the O2 hydroxyl group. In the final few femtoseconds of the simulation, the O2 hydroxyl underwent another transition to −60°, which is obscurred in Figure 4b by the graph border (see Figure 3).

As has been seen in previous simulations of complex solutes[11,13] the solvation requirements of the different functional groups in the glucose molecule have a strong structuring effect upon the immediately adjacent water molecules in the solution. Figures 5–11 illustrate atomic pair distribution functions $g(r)$, defined as[13]

$$g(r) = \frac{1}{4\pi\rho r^2}\frac{dN(r)}{dr} \quad (1)$$

for water molecules a given interatomic distance r from selected atoms in the sugar molecule, where ρ is the bulk water number

(42) De Bruyn, A.; Anteunis, M. *Carbohydr. Res.* **1976**, *47*, 311.
(43) Nishida, Y.; Ohuri, H.; Meguro, H. *Tetrahedron Lett.* **1984**, *25*, 1575.
(44) Perkins, S. J.; Johnson, L. N.; Phillips, D. C.; Dwek, R. A. *Carbohydr. Res.* **1977**, *59*, 19.
(45) Boyd, J.; Porteous, R.; Soffe, N.; Delepierre, M. *Carbohydr. Res.* **1985**, *139*, 35.
(46) Wolfe, S. *Acc. Chem. Res.* **1972**, *5*, 102.
(47) Abe, A.; Mark, J. E. *J. Am. Chem. Soc.* **1976**, *98*, 6468.
(48) Rasmussen, K. *Acta Chem. Scand., Ser. A* **1982**, *36*, 323, and references cited therein.
(49) Christofides, J. C.; Davies, D. B. *J. Chem. Soc., Chem. Commun.* **1985**, 1533.
(50) Christofides, J. C.; Davies, D. B. *J. Chem. Soc., Perkin Trans. 2* **1987**, 97.

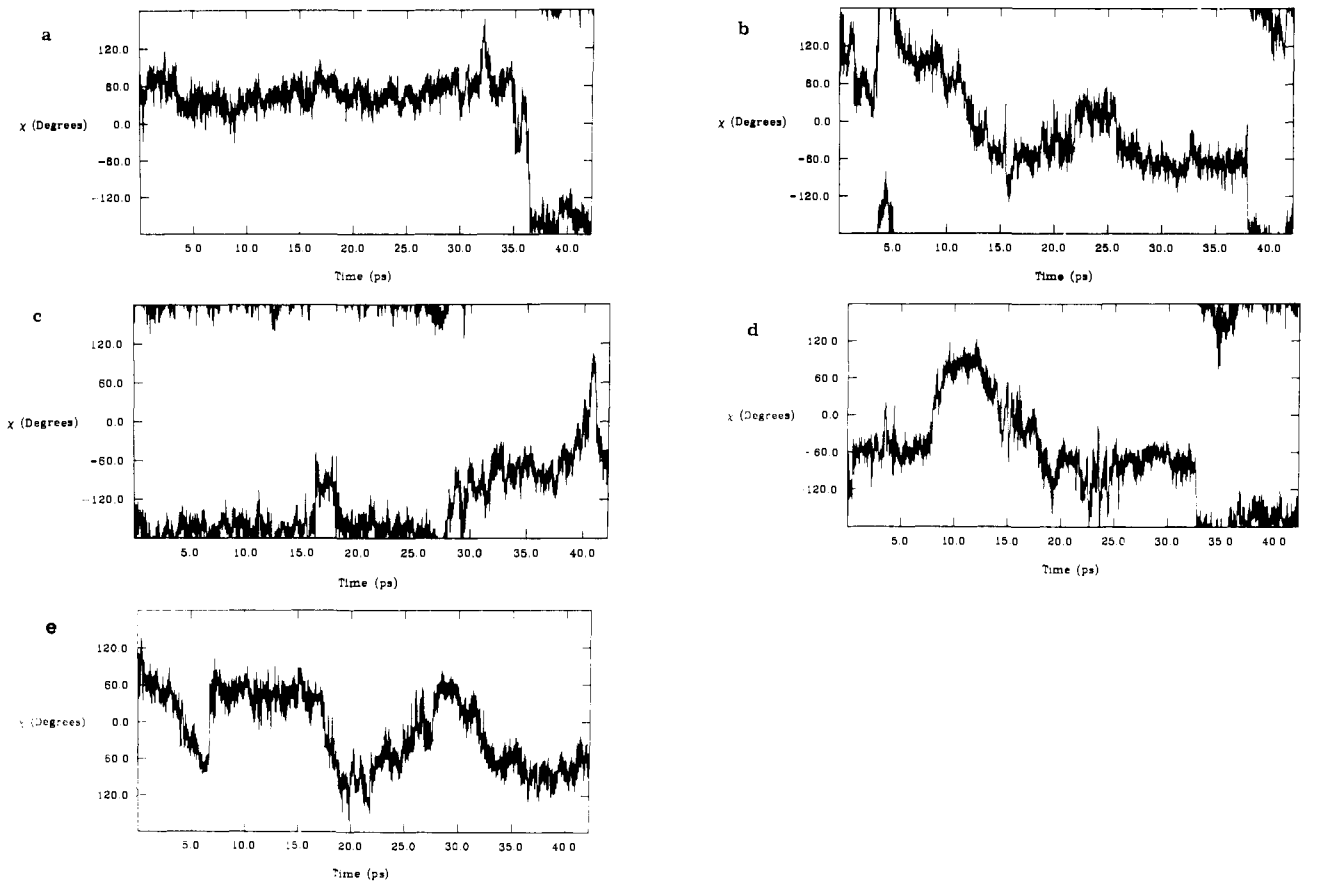

Figure 4. Histories of the dihedral angles describing the orientations of the hydroxyl groups over the entire trajectory, including the equilibration period: (a) O5-C1-O1-OH1, (b) C1-C2-O2-OH2, (c) C2-C3-O3-OH3, (d) C3-C4-O4-OH4, (e) C5-C6-O6-OH6.

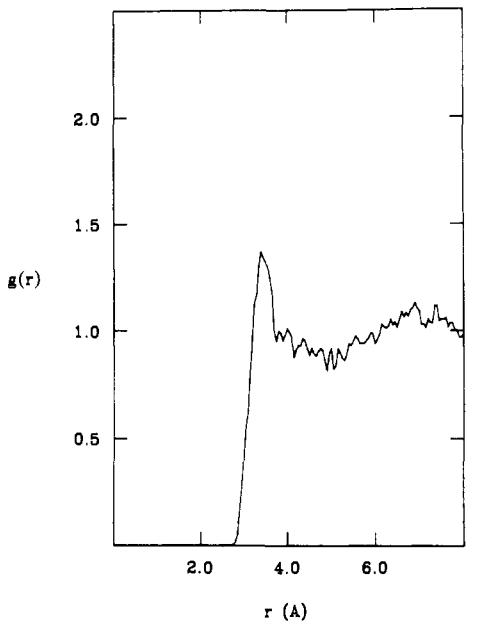

Figure 5. Water oxygen-exocyclic methylene carbon pair distribution function calculated from the data collection period of the simulation.

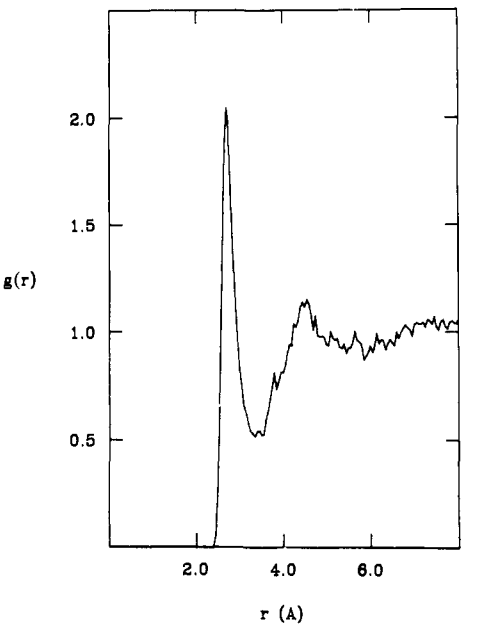

Figure 6. Water oxygen-hydroxyl oxygen O5 pair distribution function.

density. As would be expected, the distribution function for water molecules about the methylene carbon atom C6 of the exocyclic hydroxymethyl group, shown in Figure 5, exhibits nonpolar solvation behavior,[13] with a broad first peak centered at 3.4 Å, approximately the van der Waals contact distance, and 12.3 near neighbors, integrated out to the first minimum around 4.9 Å. In sharp contrast, the distributions of water oxygen atoms around the sugar hydroxyl oxygen atoms display the hydrogen-bonding behavior expected for these groups. Figure 6 illustrates an example of one of these distributions, that for the O6 hydroxyl oxygen atom. The first peak of this curve at 2.70 Å is much sharper and narrower than that of the distribution function for C6. The first minimum at approximately 3.4 Å is also much lower than in the nonpolar curve, indicating much stronger localization of the hydrogen-bonded nearest neighbors. The integral of this curve out to the first minimum gives 3.2 nearest neighbors. This value indicates that during the simulation this hydroxyl group, which can potentially serve once as a hydrogen bond donor and twice as an acceptor, had a saturated hydrogen-bonding capacity with es-

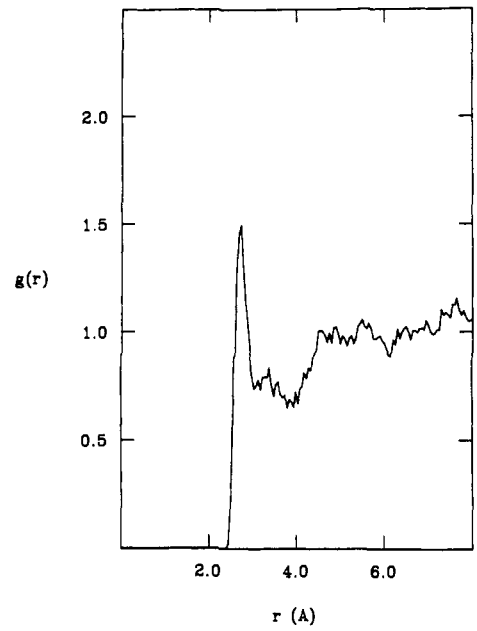

Figure 7. Water oxygen–hydroxyl oxygen O1 pair distribution function.

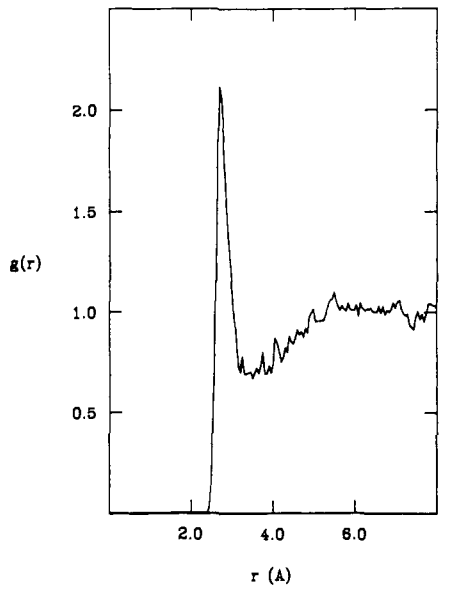

Figure 8. Water oxygen–hydroxyl oxygen O2 pair distribution function.

Table II. Characteristics of the Atomic Pair Distribution Functions for Water Oxygen Atoms around Various Atoms of the Glucose Molecule

	solute atom						
	O1	O2	O3	O4	O5	O6	C6
position of first max, Å	2.75	2.70	2.70	2.75	3.25	2.70	3.40
height of first max	1.49	2.12	2.03	1.44	0.95	2.05	1.37
near neighbors integrated out to 3.4 Å	3.0	3.6	3.6	3.1		3.2	

sentially no non-hydrogen-bonded nearest neighbors.

The pair distribution functions for the other hydroxyl groups in the sugar molecule (Figures 7–10) are generally similar to the one illustrated for O6 in Figure 6 but tend to have somewhat perturbed forms, possibly caused by the proximity of other groups. Principal characteristics of these distributions are summarized in Table II. These functions appear to fall into two groups. The distributions around the O2 and O3 hydroxyl atoms appear to be nearly identical with that for O6, and the curves for O1 and O4, while nearly identical to one another, are slightly different from those for the other three. The O2, O3, and O6 functions

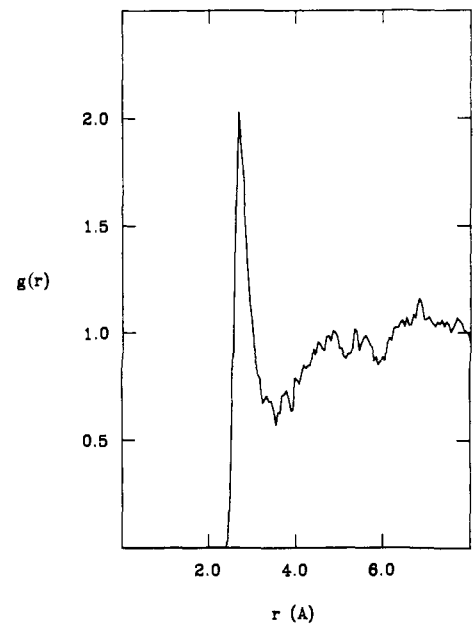

Figure 9. Water oxygen–hydroxyl oxygen O3 pair distribution function.

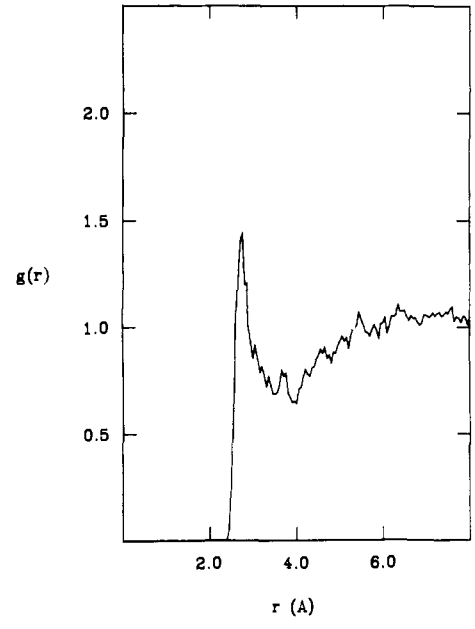

Figure 10. Water oxygen–hydroxyl oxygen O4 pair distribution function.

all have their first maximum at 2.7 Å and first minima around 3.4–3.5 Å, with first peak heights around 2.0. The distributions for O1 and O4 both have much lower first maxima and first minima that fall at slightly larger radii. With the exception of the curve for O6, none of the $g(r)$ curves exhibit significant second or third peaks, indicating little long-range structuring with these potential functions. While their first minima occur at slightly different places, the integrals of all of these curves out to 3.4 Å, the first minimum for the O6 distribution, taken as an approximate common first-minimum cutoff, are between 3 and 3.6. It is uncertain to what extent the differences between these curves are real or caused by inadequate statistics.

The close proximity of the hydroxyl groups in the sugar ring and their essentially fixed relative orientations of course means that many near-neighbor molecules are shared by more than one hydroxyl group. The requirement of simultaneously satisfying the hydrogen-bonding requirements of two groups may place greater configurational restrictions upon the hydrogen-bonded water molecules than do simplier solutes. Figure 3 illustrates one such water molecule in the final configuration of the simulation. In this illustration, the solvent molecule is quite close to the O3

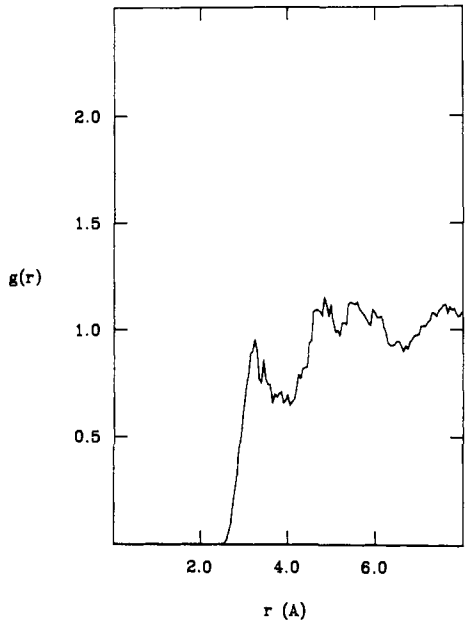

Figure 11. Water oxygen–ring oxygen pair distribution function.

group, apparently during a momentary fluctuation closer than usual to this group (the water oxygen–O3 distance in this coordinate set is only 2.56 Å, and the distance to the O2 atom is 3.03 Å). Although the O2 hydroxyl group only rotated into this conformation approximately 30 fs earlier, this water molecule has already oriented so as to be able to hydrogen bond as an acceptor for both molecules. While these hydroxyl groups are in this particular set of orientations, only a narrow range of positions and orientations would allow a single solvent molecule to hydrogen bond to both in this fashion. It would appear likely that a close correlation must exist between the reorientations of these hydroxyl groups and the motions of the first solvation shell water molecules. It is not clear, however, whether this type of shared hydrogen bonding may play any role in the anomeric equilibrium; the trajectory-averaged O1–O2 distance of 2.92 Å was found to be almost exactly the same as the O2–O3 and O3–O4 distances of 2.90 and 2.89 Å (the O4–O6 average distance in the TG conformation was also found to be 2.89 Å). However, the relative orientations could well be important and may have contributed to the different characters for the pair distribution functions for water molecules around the O1 and O4 atoms. This possible effect should be examined in simulations of other epimers of glucose.

The solvation of the ring oxygen atom O5 is quite different from that of the hydroxyl oxygens. Due to its lower atomic partial charge (−0.4 vs -0.6_5), this atom does not compete successfully for hydrogen-bonding partners. The pair distribution function for this atom is displayed in Figure 11. The first peak in this function is located at a much larger distance, at 3.25 Å, and is weaker and broader than those for the hydrogen-bonded oxygen atoms, not even reaching bulk density. The integral of this curve out to the first minimum around 3.9 Å is approximately 3.8 neighbors. This type of distribution indicates considerably less localization of nearby water molecules than is found around the hydroxyl groups.

The various solute functional groups also impose orientational order or structuring upon the nearest-neighbor water molecules. Figure 12 displays the orientational distribution function $P(\cos\theta)$ for water molecules near the C6 carbon atom of the exocyclic hydroxymethyl group. This function is the integrally normalized probability of finding an angle θ between each of the O–H bond vectors in the nearest-neighbor water molecules and the vector defined by the line from the C6 atom to the oxygen of that water molecule.[13] For this purpose, the nearest neighbor distance is defined as the distance of the first minimum in the pair distribution function (4.9 Å from C6). All water molecules within this cutoff distance of the carbon atom have been included in the averaging to produce Figure 12. The behavior displayed by this distribution

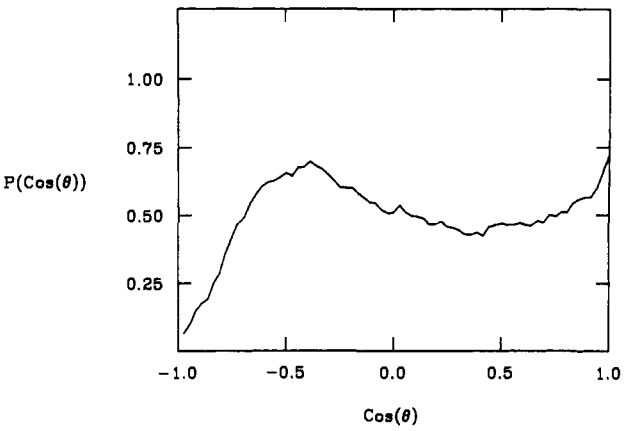

Figure 12. Distribution of orientations for those water molecules adjacent to the methylene C6 atom.

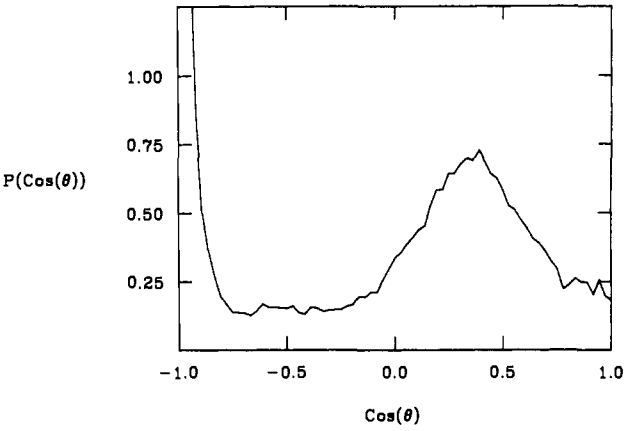

Figure 13. Distribution of orientations for those water molecules adjacent to the O3 hydroxyl oxygen atom.

is typical of hydrophobic solvation,[13] with a peak at +1 indicating a tendency for one of the hydrogen atoms to point directly away from the nonpolar group. The broad peak from around −0.2 to −0.7 is the consequence of the tetrahedral molecular geometry of the rigid SPC water molecules; if one of the hydrogens is pointing directly away from the methylene group, the other water OH bond vector must be making a tetrahedral angle ($\cos\theta = -0.33$) with the C–O vector. The deep minimum at −1 indicates that there is little probability of a hydrogen atom pointing directly at the methylene group. This structuring behavior is adopted as the "best" way for water molecules to solvate a nonpolar group of small radius without sacrificing any hydrogen bonds. The cost of this structuring is entropic as the configurational freedom of the water molecules is restricted.[13]

Similar distribution functions can be computed for the water molecules around the various hydroxyl oxygen atoms of the sugar. Figure 13 illustrates this function for the water molecules within 3.5 Å of the O3 atom of the solute. The behavior displayed by this distribution is typical of hydrogen bonding. The strong peak at −1 indicates that one of the hydrogen atoms of donor near-neighbor water molecuis is essentially pointing directly at the hydroxyl oxygen atom. The broad secondary peak around +0.4 again results from the tetrahedral geometry of the rigid SPC water molecules. This orientational distribution function for the ring O5 atom, illustrated in Figure 14, displays an almost flat distribution of angles, indicating little orientational preference for these molecules, as the result of the lack of hydrogen bonds to the ring oxygen.

The orientational distribution functions calculated from the simulation for the O1, O4, and O6 hydroxyl oxygens are all essentially identical with the curve for O3 displayed in Figure 13. This function for the O2 hydroxyl oxygen, however, illustrated in Figure 15, is substantially perturbed. This distribution is almost flat, with only a slight preference for the typical hydrogen bond

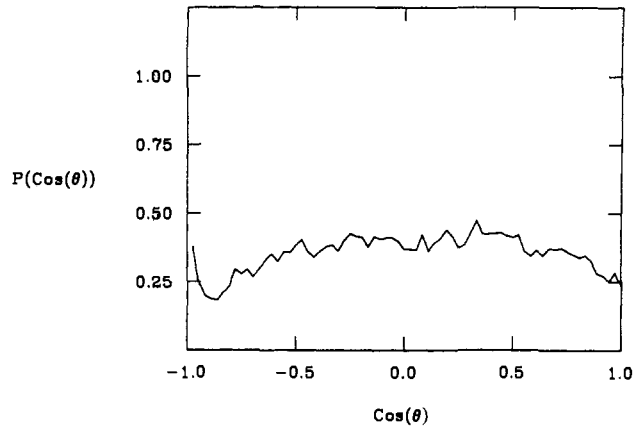

Figure 14. Distribution of orientations for those water molecules adjacent to the ring oxygen atom.

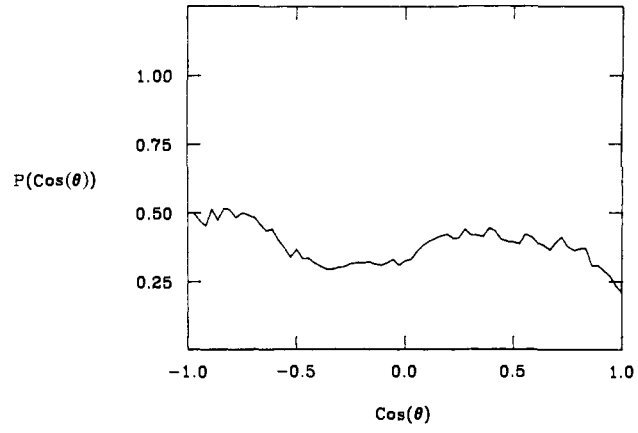

Figure 15. Distribution of orientations for those water molecules adjacent to the O2 hydroxyl oxygen atom, averaged over the entire data collection period of the simulation.

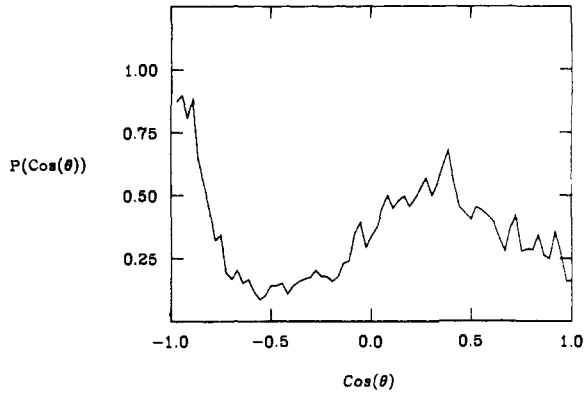

Figure 16. Distribution of orientations for those water molecules adjacent to the O2 hydroxyl oxygen atom, averaged over the final 6 ps of the simulation.

orientation. Only during the final few picoseconds of the simulation, when this O2 hydroxyl had rotated to the ±180° well (Figure 4b), did the adjacent water molecules reorient to the more "ideal" hydrogen-bonding pattern (Figure 16 illustrates this orientational distribution for water molecules near the O2 atom calculated from the final 6 ps of the simulation). The pair distribution function for water oxygen atoms around O2, however, is quite ordinary throughout the simulation (Figure 8), indicating three hydrogen bond partners sharply localized radially, even if their orientations are not optimal for an extended hydrogen bond network during much of the simulation. Figure 17 shows selected water molecules close to the O2 atom for an instantaneous configuration from the middle of the simulation. As can be seen from this figure, the O2 hydroxyl can form a strong hydrogen bond

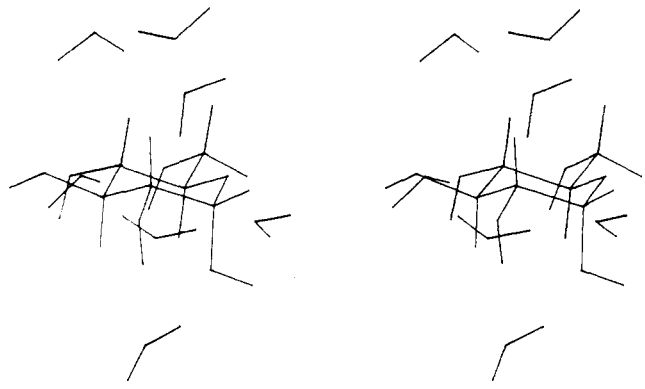

Figure 17. Stereoview of a typical configuration for the early portion of the simulation, including selected water molecules adjacent to the O2 hydroxyl group.

as a donor, even though the OH vectors of the water molecule to which it is hydrogen-bonded may be at an uncharacteristic angle as the result of the hydrogen-bonding requirements of its neighboring molecules. Two other nearby water molecules, at approximately the hydrogen bond distance, have favorable Coulombic interactions of their hydrogen atoms with the O2 hydroxyl oxygen, but apparently due to their other hydrogen-bonding requirements, neither of these is oriented so as to point the bond vector directly at O2.

The perturbation in angular orientation around O2 is quite possibly an artifact of insufficient simulation time, but it is tempting to speculate as to whether it may be a reflection of the anomeric structure of the molecule. If the perturbation in solvent ordering around this group was caused by the axial orientation of the C1 hydroxyl, then the effect could possibly be related to the anomeric preference for β in glucose. In the α-anomer, the axial position of the anomeric hydroxyl group also means that the aliphatic hydrogen on the C1 carbon is pointing "up" relative to the mean plane of the ring, as is also the case for the aliphatic hydrogen on the C2 carbon atom (see Figures 1 and 3). This adjacent positioning of the two methylene hydrogen atoms creates an extended region of hydrophobicity, which is closer to the O2 hydroxyl group than to the O1 group. The hydrophobic hydration of these CH groups imposes structuring on their first solvation shell water molecules, some of which are also nearest neighbors of the O2 hydroxyl oxygen atom. The quite different structural behavior of these water molecules may be the reason for the perturbed orientational distribution for water molecules around O2, at least for two of the three principal orientations of this hydroxyl group. Although this perturbation is a small effect, it is possible that it could be the basis for the differing free energies of the α- and β-anomers if their energy difference is indeed caused by solution effects.

As can be seen from the pair distribution functions for water molecules about the sugar atoms, different functional groups in the molecule have differing effects upon the solvent. The relatively sharp first peaks in these functions for the hydroxyl oxygen atoms, with their deep first minima, indicate that the water molecules near to these groups are well localized and that these interaction or "binding" sites are almost always occupied by water molecules. This localization is dynamic in character, however, and does not mean that specific water molecules are "bound" to the solute in a kinetic sense.[51] Throughout the simulation, these first solvation shell water molecules are exchanging by slow diffusive motion with other molecules from the bulk or solvation shells of other solute atoms. Figure 18 illustrates some examples of this diffusive exchange. This figure shows the separation distance from the O4 atom to the oxygen atom of four selected water molecules during the initial 16 ps of data collection in the simulation. Two of these molecules were initially quite close to the oxygen atom, making hydrogen bonds to the hydroxyl group (Figures 18a,d). As the

(51) Kuntz, I. D.; Kauzmann, W. *Adv. Protein Chem.* **1974**, *28*, 239.

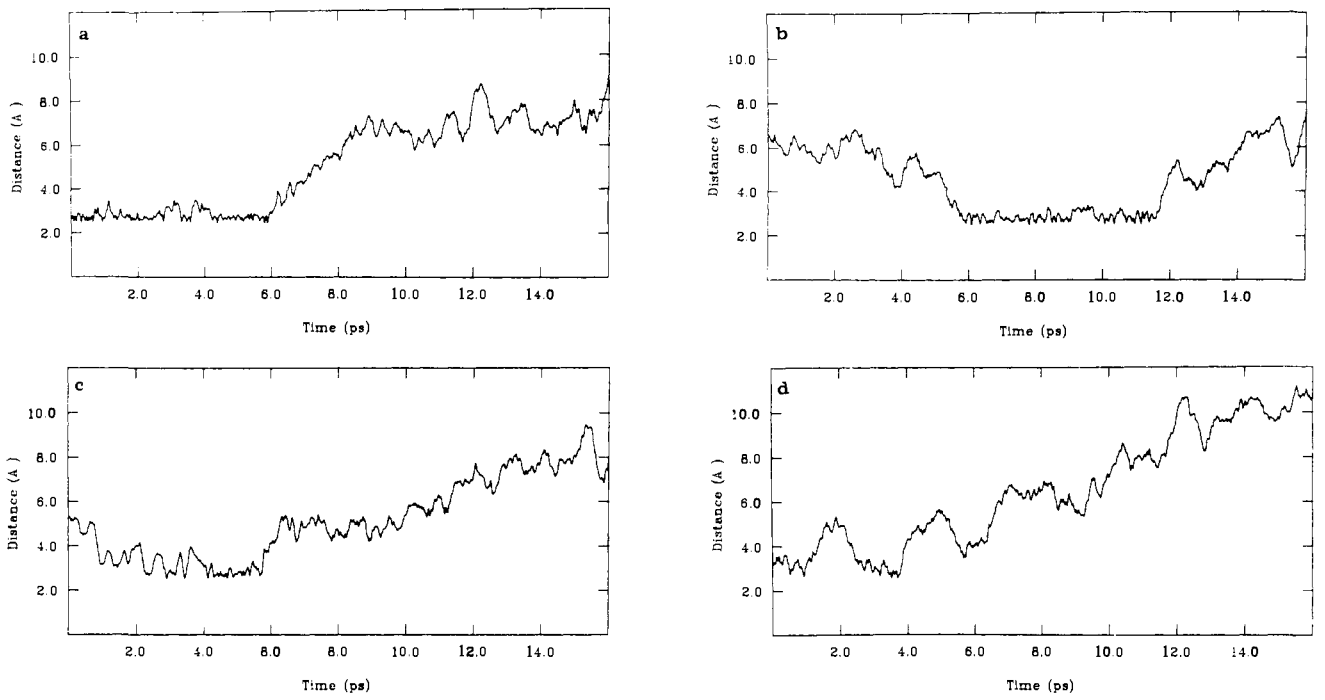

Figure 18. Plots of the distance, as a function of time, for the oxygen atoms of several different water molecules from the O4 atom of the sugar molecule. As hydrogen-bonded partners escape into the solution, they are simultaneously replaced by other molecules.

water molecule of Figure 18a escaped around 6 ps into the data collection period, it was simultaneously replaced by the water molecule of Figure 18b, which diffused in from the bulk region. This second molecule also escaped around 12 ps into the simulation. A similar exchanging pair is shown in Figures 18c,d, where the molecule of Figure 18d made two returns before completely escaping far into the bulk solvent. Quantitating residence lifetimes for this type of behavior in a statistically meaningful way that will not depend upon definitions is difficult, but it appears qualitatively that typical residence times are on the order of a few picoseconds (<10 ps).

In principle, diffusion coefficients for water molecules adjacent to specific functional groups in the solute can be estimated from a simulation such as this by computing either the center-of-mass velocity autocorrelation function or the mean-square displacement of those near-neighbor solvent molecules sorted by class.[13,52] In practice, such a calculation is difficult from a short simulation, since not only is the simulation time relatively brief, but when the solvent is partitioned into subensembles around each functional group, each subensemble contains only a very small number of molecules. Operationally, the calculation of such mean-square displacements is complex, since the identities of the molecules to be included in the subensembles around each functional group are changing as they diffuse in and out of range, requiring special treatment in the data collection and normalization to avoid biasing the calculated numbers by excluding the faster diffusing members of the ensemble.

Center-of-mass mean-square displacements as a function of time were computed from the present simulation data for various subsets of the water molecules, including all those in the bulk solution, and for those molecules around each of the oxygen atoms. Figure 19 displays the mean-square displacements of those water molecules within 3.5 Å of the O1, O2, and O4 hydroxyl oxygens, as well as for those molecules classified as being in the "bulk" solvent (that is, more than 3.5 Å from any polar atom in the solute and more than 4.5 Å from the nonpolar exocyclic methylene group). Translational diffusion coefficients for the water molecules in each of these classes, estimated from a least-squares analysis of the limiting slopes, are listed in Table III. As can be seen, the translational freedom of waters adjacent to the hydroxyl oxygen

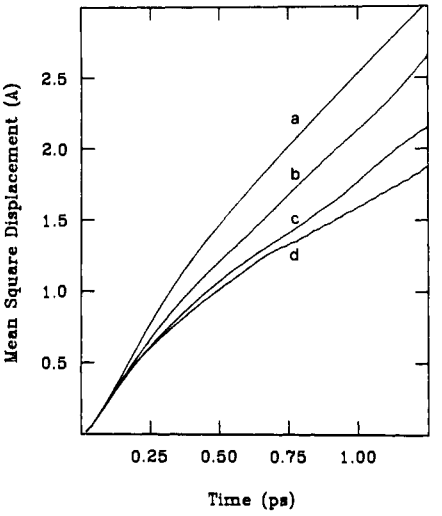

Figure 19. Mean-square displacements for water molecule center-of-mass translation for several classes of solvent molecules: (a) bulk; (b) those water molecules adjacent to O1; (c) those water molecules adjacent to O2; (d) those water molecules adjacent to O4.

Table III. Translational Diffusion Coefficients for Those Water Molecules Adjacent to Various Groups in the Solute

	class							
	O1	O2	O3	O4	O5	O6	C6	bulk
D, 10^{-5} cm^2/s	3.2	2.4	3.1	1.8	2.1	2.1	4.1	3.5

atoms is somewhat restricted relative to the bulk water molecules. This result is consistent with previous solution simulation studies.[13,53] From the well-converged bulk curve, the bulk translational diffusion coefficient is estimated to be 3.5×10^{-5} cm^2/s, compared to the value of 3.6×10^{-5} cm^2/s reported for pure SPC water at approximately this temperature as calculated from a 12-ps simulation.[35] The diffusion coefficient for those water molecules adjacent to O1 was found to be only slightly smaller than that of the bulk water molecules and essentially identical with that

(52) Zichi, D. A.; Rossky, P. J. *J. Chem. Phys.* **1986**, *84*, 2814.

(53) Brady, J. W.; Karplus, M., unpublished results.

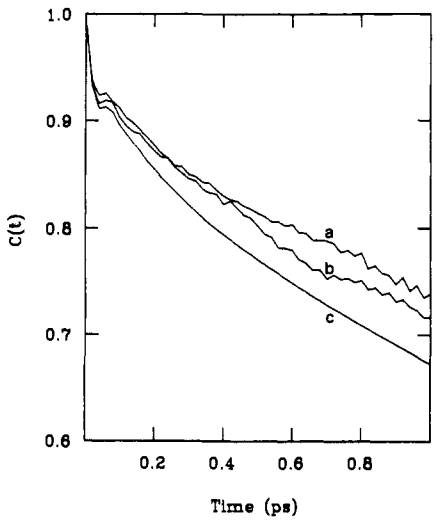

Figure 20. Rotational correlation function C_1 for several classes of solvent molecules: (a) those water molecules adjacent to C6; (b) those water molecules adjacent to O6; (c) bulk solvent molecules.

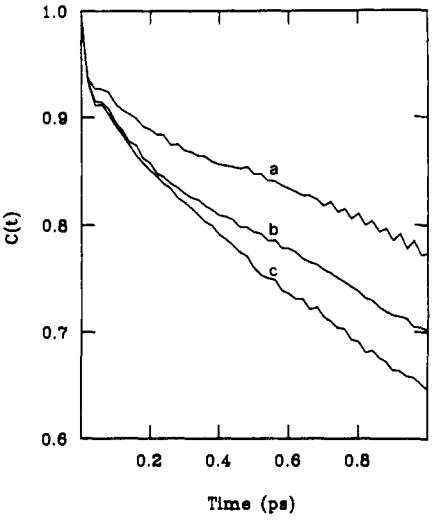

Figure 21. Rotational correlation function C_1 for several classes of solvent molecules: (a) those water molecules adjacent to O5; (b) those water molecules adjacent to O2; (c) those water molecules adjacent to O1.

found for those water molecules adjacent to the O3 atom. Those water molecules adjacent to the O2, O4, O5, and O6 atoms were found to be substantially affected by the presence of the solute. Surprisingly, water molecules within 4.5 Å of the exocyclic CH_2 group were found to be diffusing somewhat faster than the bulk molecules, with a diffusion coefficient of 4.1×10^{-5} cm^2/s.

The rotational diffusion of the water molecules, also classified according to which functional groups of the solute they are closest to, was characterized by computing time correlation functions for the molecular dipole direction[13]

$$C_l(t) = \langle P_l(\hat{\mu}(t)\cdot\hat{\mu}(0))\rangle \quad (2)$$

where P_l is the Legendre polynomial of order l. For $l = 1$

$$C_1(t) = \langle \cos\theta \rangle \quad (3)$$

This function is plotted in Figures 20 and 21 for water molecules adjacent to several of the solute groups, as well as for the bulk water molecules. The water molecules near O1 were found to be rotating about as fast as those in the bulk solvent, as was the case for their translational diffusion as well, while those water molecules near the O5 ring oxygen were substantially slowed in their rotational motions, as was also the case for their translational diffusion. The water molecules near the O2 atom, as well as those near the C6 methylene atom, exhibited rotational behaviors between these extremes, rotating more slowly than those solvent molecules adjacent to O1.

Since there is no obvious relationship between those functional groups which have similar diffusion coefficients for their immediately neighboring water molecules or any correlation with the observed groupings of pair distribution functions, it must be questioned whether there is any significance to the variations other than statistical fluctuations due to inadequate sampling. For example, previous simulations[13,52] as well as experimental studies[54] have found that water molecules adjacent to methyl groups are more restricted in their translational diffusion than those of the bulk solvent, in contrast to the results found here. Previous experience with a far longer simulation (>100 ps) of a less complex solute (the alanine "dipeptide") indicates that these diffusional properties require extensive simulation time for convergence.[53] It would appear, then, that in the present simulation the results are not yet statistically converged and that these values cannot be considered to be definitive. This view is supported by the fact that the values calculated from shorter subsets of the present trajectory, while in the same range, were individually very different between subsets, with different orderings and groupings. Apparently, a much longer simulation will be needed to definitively quantitate these diffusion coefficients.

(54) Goldammer, E. V.; Hertz, H. G. *J. Phys. Chem.* **1970**, *74*, 3734.

IV. Conclusions

From these simulations, the behavior of α-D-glucopyranose in aqueous solution would appear to be generally consistent with the behavior observed in previous simulations of complex solutes.[10-15] Solvation was observed to have very little effect upon the basic conformation of the pyranoid ring. It is perhaps surprising that the primary alcohol group spontaneously underwent a transition to the TG conformation in solution, as also happened in vacuum simulations. This transition in vacuo is favored since the TG conformation allows the molecule to make an internal hydrogen bond. In this context, the absence of this conformation in crystal structures is of little relevance, since crystal structures are dominated by intermolecular hydrogen bonds to crystal neighbors. The presence of this conformation in the present simulation, however, seems to contradict inferences from NMR studies of glucose in aqueous solution,[42-44] where alternate hydrogen bond partners compete with the intramolecular hydrogen bond. The significance of this result is unclear; it may indicate a physical phenomenon or may be the result of inaccuracy in the potential energy function, particularly in the treatment of the "gauche effect". It is also possible that the long residence in the TG well in this simulation was a statistical accident, created by the equilibration procedure and maintained by the heights of the barriers to transition rather than the relative energy differences of the wells, and that a much longer simulation, or an ensemble of shorter simulations, would find transitions to the other forms. Further simulations will be needed to resolve this question.

In order to adequately investigate any structural or dynamical basis for the anomeric partitioning, it will of course be necessary to perform an equivalent MD simulation of β-D-glucopyranose for comparison. It has been proposed that the equatorial distribution of hydroxyl groups in the β-anomer results in a distribution of oxygen positions that closely matches the arrangement of oxygen atoms in the crystalline ice I*h* lattice, resulting in a better hydrogen-bonding "fit" to the presumed liquid solvent structure than in the case of the axial C1 hydroxyl in the α-anomer.[20,21] This model apparently assumes a greater degree of long-range icelike tetrahedral ordering in liquid water than has been observed in simulations of pure liquid water. The simulations reported here appear to offer little direct support for this model for the explanation of the equilibrium anomeric concentrations. However, the observed perturbation of the structuring of water molecules adjacent to the O2 atom is intriguing and, if this result is not an artifact of insufficient simulation time, may be related to the determination of the anomeric ratio. It is possible that the proximity of the strongly hydrated axial C1 hydroxyl group,

pointing "down" relative to the mean ring plane, as is the equatorial C2 hydroxyl, places constraints on the likely orientations of the O2 near neighbors. In this context, it is worth noting that, for all of the pyranoid pentose and hexose sugars, which exist predominantly in the $^4C_1$ conformation, the preferred anomer in aqueous solution is that form which has the anomeric, O1 hydroxyl and the O2 hydroxyl groups on opposite sides of the mean plane of the ring,[55] as is the case in β-D-glucopyranose. Since the free energy difference between the two forms in water at 300 K is only approximately 0.34 kcal/mol, it is probable that if this difference is due to solvation effects, much longer simulations will be necessary for such a small difference to emerge from the background statistical noise of the data.

Acknowledgment. I thank M. Karplus, S. N. Ha, L. Madsen, B. R. Brooks, and Tran Vinh for helpful discussions. This work was supported in part by NIH Grant No. GM34970 and by Hatch Project 143-7433, USDA. Figures 3 and 17 were prepared using the HYDRA molecular graphics program written by R. E. Hubbard of the University of York.

Registry No. α-D-Glucopyranose, 492-62-6.

(55) Shallenberger, R. S. *Advanced Sugar Chemistry*; AVI Publishing Co.: Westport, CT, 1982.

Early Stages of Diborane Pyrolysis: A Computational Study

John F. Stanton,*,†,‡ William N. Lipscomb,† and Rodney J. Bartlett§

Contribution from the Gibbs Chemical Laboratory, Harvard University, Cambridge, Massachusetts 02138, and Quantum Theory Project, Departments of Chemistry and Physics, University of Florida, Gainesville, Florida 32611. *Received November 25, 1988*

Abstract: Methods of many-body perturbation theory and the coupled-cluster approximation are applied to a study of two elementary processes believed to play a role in the pyrolysis of diborane, $BH_3 + B_2H_6 \rightarrow B_3H_9$ (II) and $B_3H_9 \rightarrow B_3H_7 + H_2$ (III). Results indicate that the reaction pathway for II proceeds through a transition state stabilized by a donation–backdonation interaction reminiscent of that involved in hydroboration and that the activation and reaction enthalpies (at 400 K) for this process are approximately 14 and −5 kcal/mol, respectively. Loss of molecular hydrogen from the triborane(9) formed in II appears to occur with a negligible kinetic barrier, leading to an isomer of B_3H_7 with C_{2v} symmetry. Significantly, a C_s form of triborane(7) is found to be 4 kcal/mol more stable than the C_{2v} isomer. Thus, the theoretical reaction enthalpy for III of +9 kcal/mol represents an approximate upper limit to the activation energy for the most favorable route of hydrogen loss from B_3H_9, suggesting that the barrier for this process is much lower than has heretofore been assumed. This result, coupled with the probability that triborane(9) is formed with ≈20 kcal/mol of excess internal energy, casts doubt over the common belief that step III is the slow step in the uncatalyzed pyrolysis of diborane. Relative rates for thermolysis of B_2H_6 and B_2D_6 are also computed from the theoretical energies, harmonic force fields, and structures. Regardless of which step is assumed to be rate-determining, resulting values of k_H/k_D (1.7 and 2.4 for II and III, respectively) are substantially smaller than the observed ratio of ≈5. Possible sources of this discrepancy are discussed.

I. Introduction

The thermal interconversion of the boranes is an extremely complex process. Although direct pyrolysis of diborane was used by Stock in the 1920's to synthesize a number of larger boron hydrides,[1] little is known about the individual reactions which participate in this process. Nearly forty years after the first kinetic studies appeared in the literature,[2] even the initial steps of the reaction sequence have not been clearly established. Exemplary studies by the groups of Schaeffer[3] and Fehlner[4] have produced evidence which suggests that the overall conversion is initiated by the symmetric dissociation of diborane, followed by addition of a borane fragment to unreacted diborane with subsequent elimination of molecular hydrogen.

$$B_2H_6 \rightarrow 2BH_3 \quad \text{(I)}$$

$$B_2H_6 + BH_3 \rightarrow B_3H_9 \quad \text{(II)}$$

$$B_3H_9 \rightarrow B_3H_7 + H_2 \quad \text{(III)}$$

The kinetics of this process are 3/2 order in diborane, implicating either II or III as the rate-determining step,[2] with respective rate expressions

$$\text{Rate} = k_{II}K_I^{1/2}[B_2H_6]^{3/2} \quad (1)$$

and

$$\text{Rate} = k_{III}K_{II}K_I^{1/2}[B_2H_6]^{3/2} \quad (2)$$

where K_j is the equilibrium constant for reaction j. When perdeuterated diborane is pyrolyzed, a very large retardation of the rate is observed ($k_H/k_D \approx 5$).[3a] Since vibrational contributions to energy differences typically favor products of unimolecular dissociations and are necessarily smaller (in magnitude) for reactions involving perdeuterated species, one would expect a larger value of k_H/k_D if III is the slowest step under the reaction conditions, as pointed out by Enrione and Schaeffer.[3a] Effective activation enthalpies for B_2H_6 pyrolysis can be deduced from eq 1 and 2 and are

$$H_{eff}^{\ddagger} = 0.5\Delta H_I^{\ddagger} + H_{II}^{\ddagger} \quad (3)$$

if II limits the rate and

$$H_{eff}^{\ddagger} = 0.5\Delta H_I^{\ddagger} + \Delta H_{II}^{\ddagger} + H_{III}^{\ddagger} \quad (4)$$

if loss of molecular hydrogen from triborane(9) is the slow step.

† Harvard University.
‡ AT&T Foundation Fellow.
§ University of Florida.

(1) Stock, A. *Hydrides of Boron and Silicon*, Cornell University Press: Ithaca, NY, 1933.
(2) Early kinetic studies of diborane pyrolysis are summarized in the following: *Production of the Boranes and Related Research*, Holzmann, R. T., Ed.; Academic Press: New York, 1967; pp 90-115. More recent studies are referenced in the following: Greenwood, N. N.; Greatrex R. *Pure Appl. Chem.* **1987**, *59*, 857.
(3) (a) Enrione, R. E.; Schaeffer, R. *Inorg. Nucl. Chem.* **1961**, *18*, 103. (b) Brennan, G. L.; Schaeffer, R. *Inorg. Nucl. Chem.* **1961**, *20*, 205.
(4) Fehlner, T. P. In *Boron Hydride Chemistry*; Muetterties, E. L., Ed.; Academic Press: New York, 1975; pp 175–196, and references therein.

0002-7863/89/1511-5165$01.50/0